Status of the ATLAS Pixel Detector at the LHC and its performance after three years of operation

PIXEL2012

Inawashiro – 3-7 September 2012

Attilio Andreazza

Università di Milano and INFN

for the ATLAS Collaboration.

With special thanks to P. Morettini, K. Lantsch and B. Di Girolamo

Layout

- The ATLAS Detector at the LHC
- The Pixel Detector
- In situ calibrations and performance
- Status and operation in 2012
  - Operational efficiency
  - Radiation effects on silicon and electronics
- Tracking performances
- Summary and perspectives

Some preview of the posters:

- **Track and vertex reconstruction in the ATLAS Inner Detector**
- **Monitoring radiation damage in the ATLAS Pixel Detector**
- **Neural network based cluster creation in the ATLAS silicon Pixel Detector**

A Toroidal LHC Apparatus

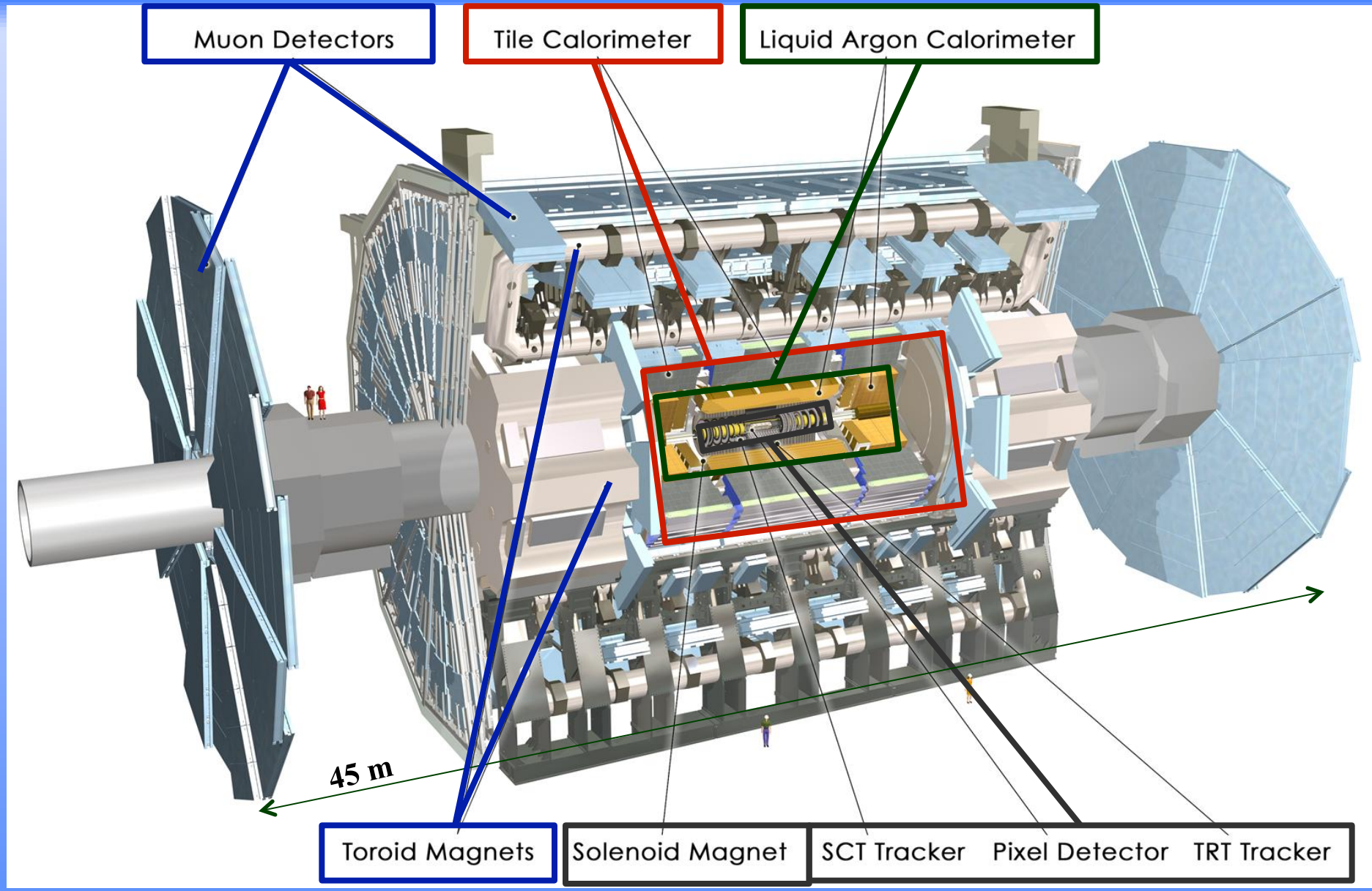

Trigger and data processing

Three level trigger system:

- Level 1, hardware
  - 2.5 μs latency
- Level 2 + Event Filter, software
- **Prescales adjusted according to instantaneous beam conditions**
- **Sustained output rate up to 400 Hz**

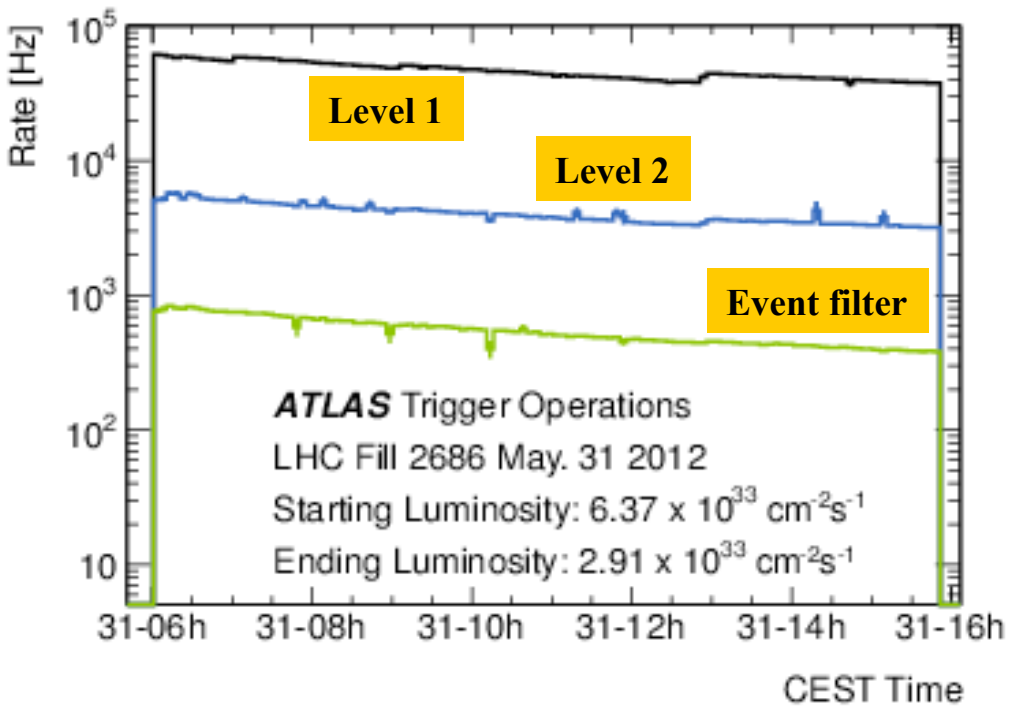

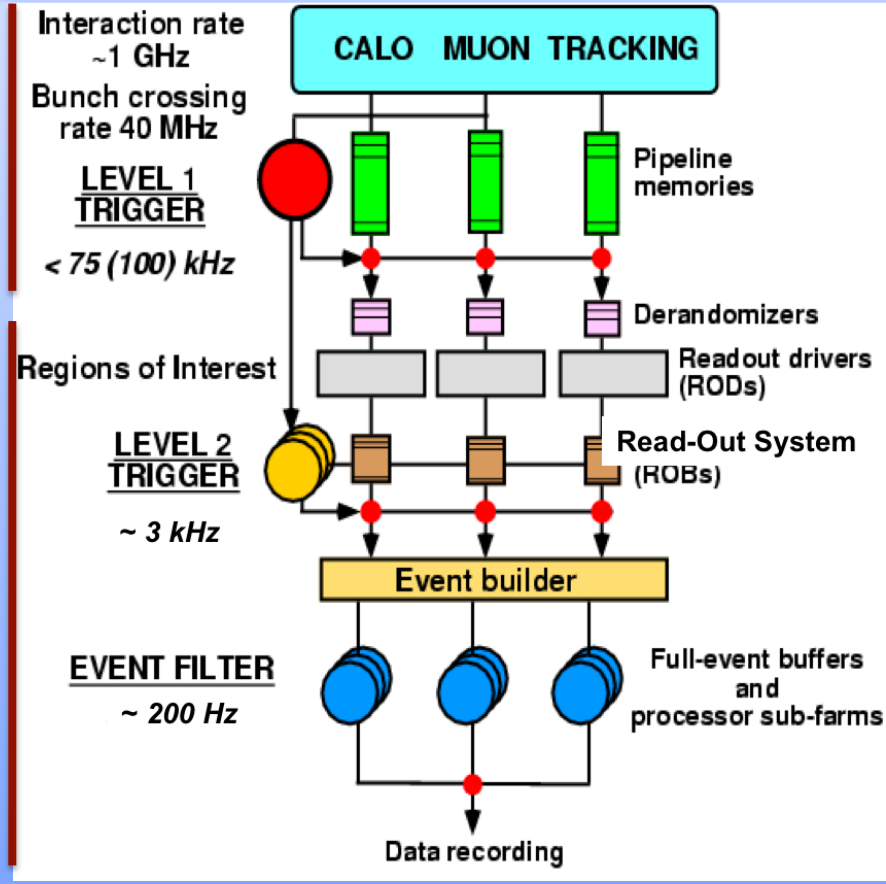

Running conditions

- LHC is performing extremely well
  - Luminosity > 7×10^{33} $cm^{-2}s^{-1}$ almost at its design value.
  - Bunch spacing at 50 ns
    ⇒ a lot of pile-up!

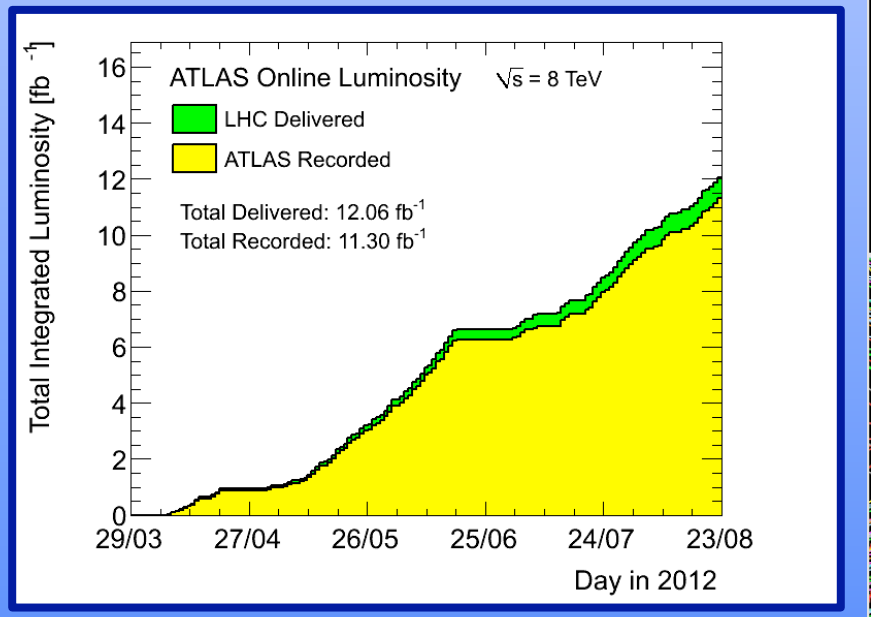

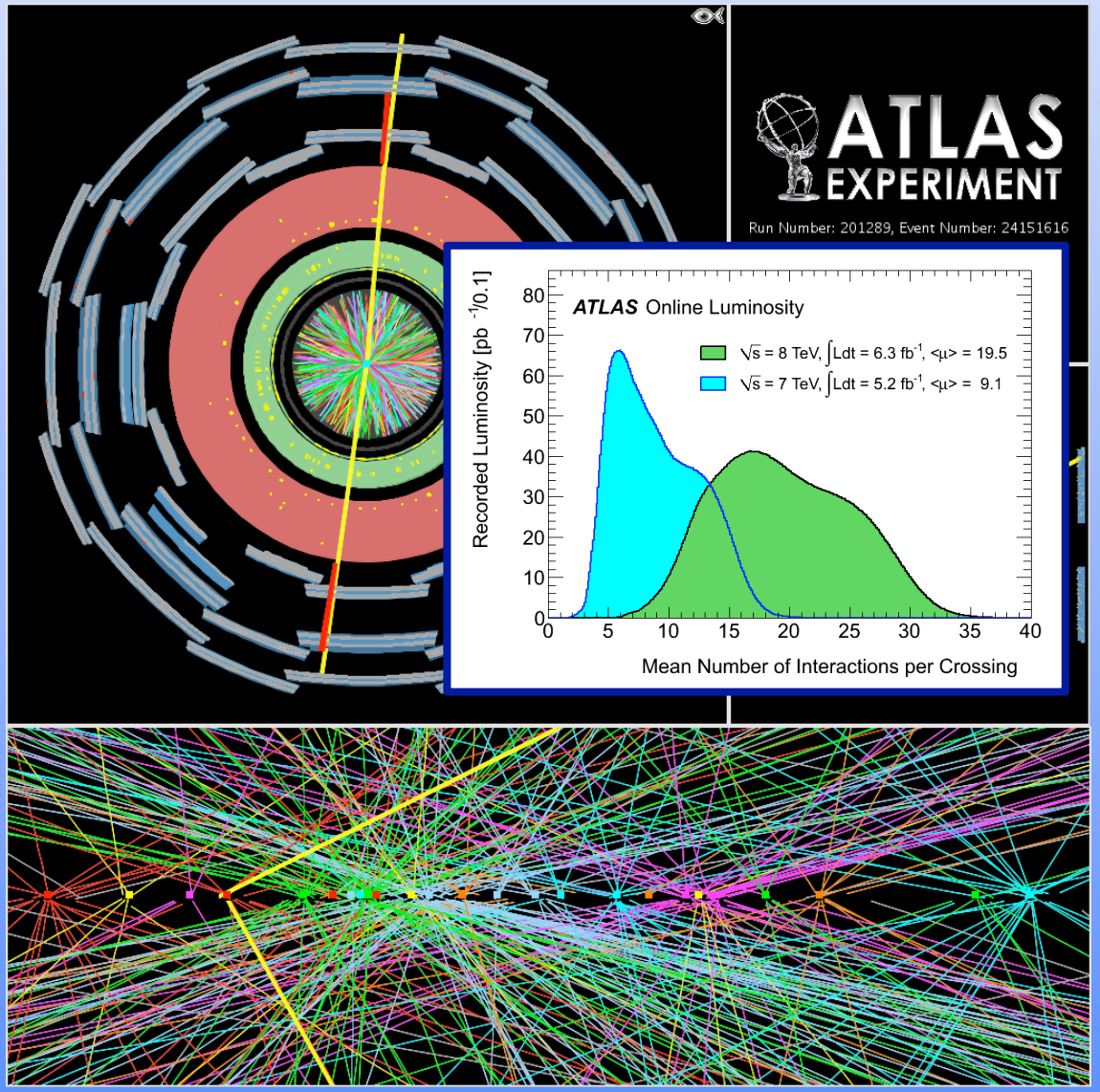

ATLAS Inner Detector

- Composite tracking system:
  - Transition Radiation Tracker
  - Silicon Strips: 80 μm pitch/stereo
  - Silicon Pixels: 50 μm × 400 μm
- 2 T solenoidal magnetic field
- Track reconstruction:
  - Acceptance $|\eta|<2.5$ ($|\eta|<2$ for TRT)
  - Reconstruction possible down to $p_T \approx 100$ MeV

See Kenji Hamano's poster for ATLAS tracking performance

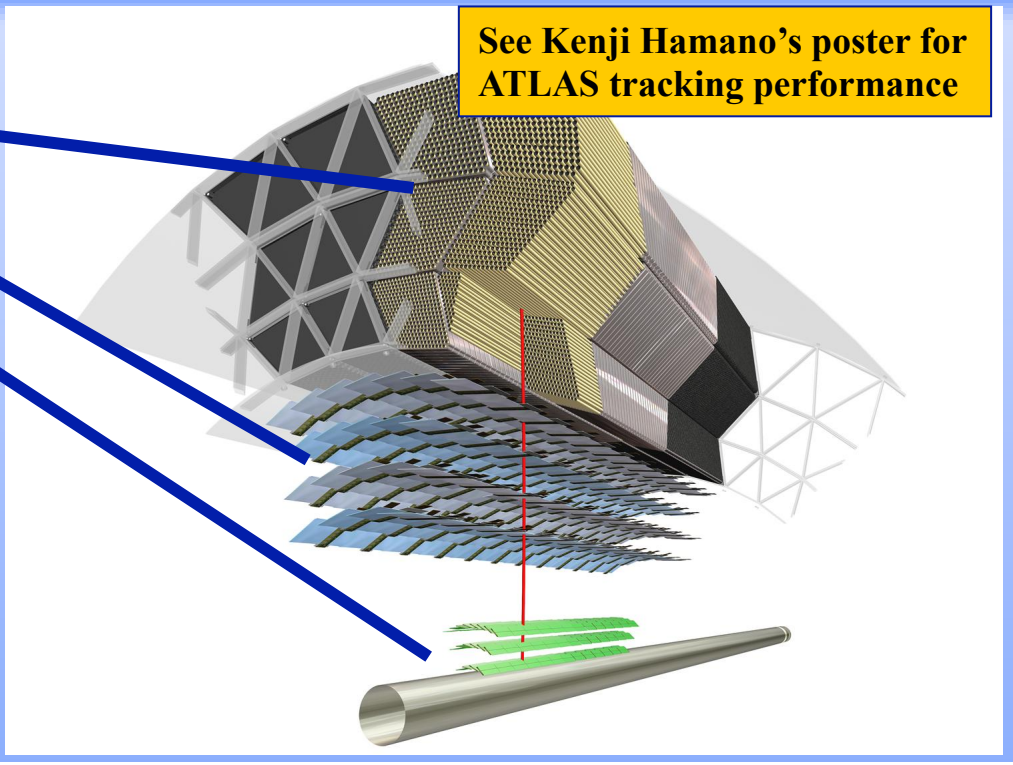

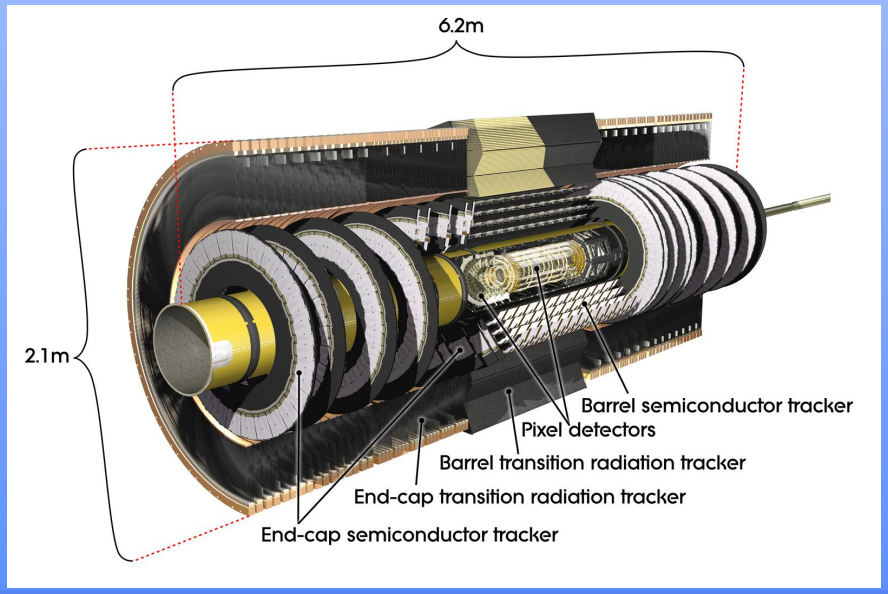

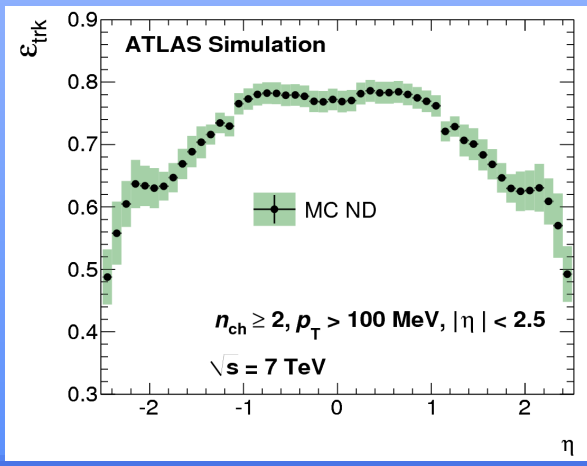

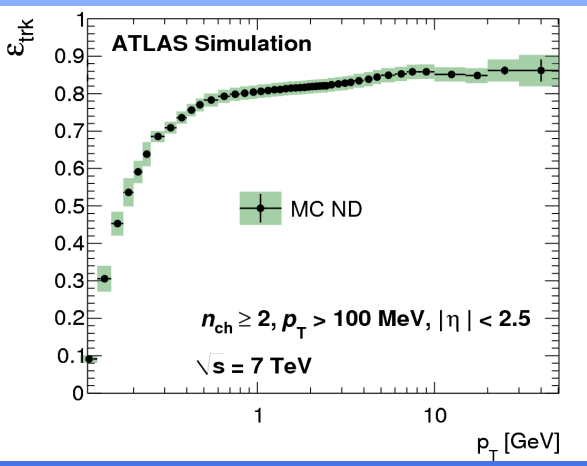

The ATLAS Pixel Detector

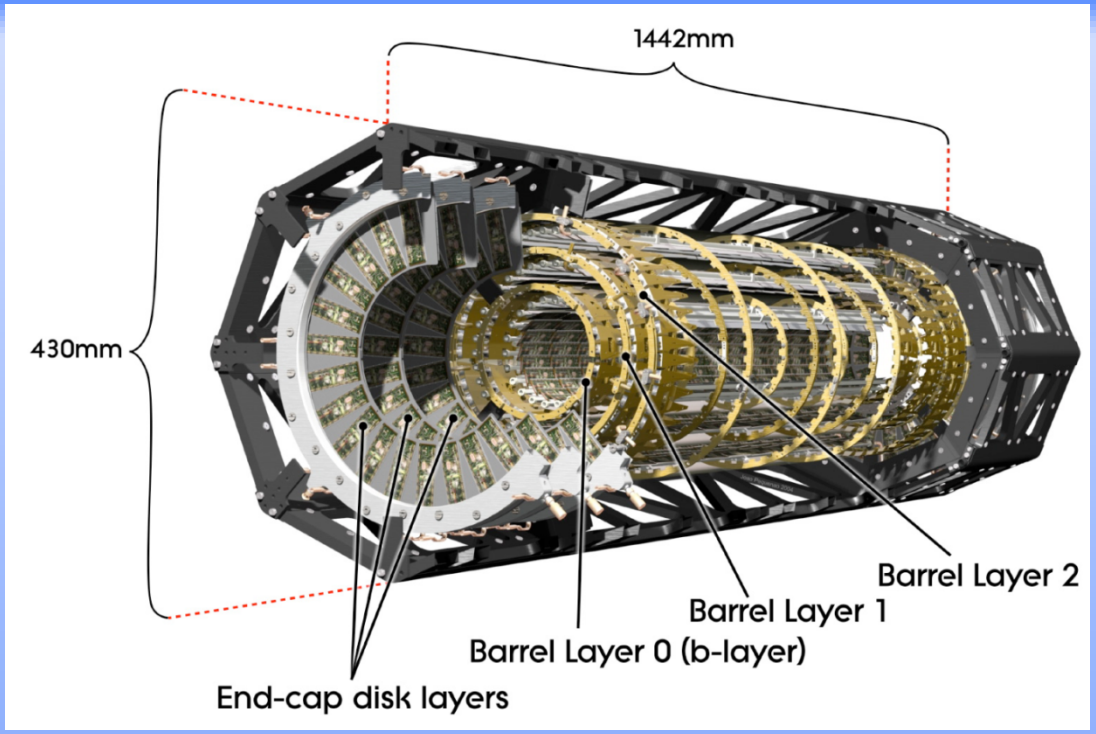

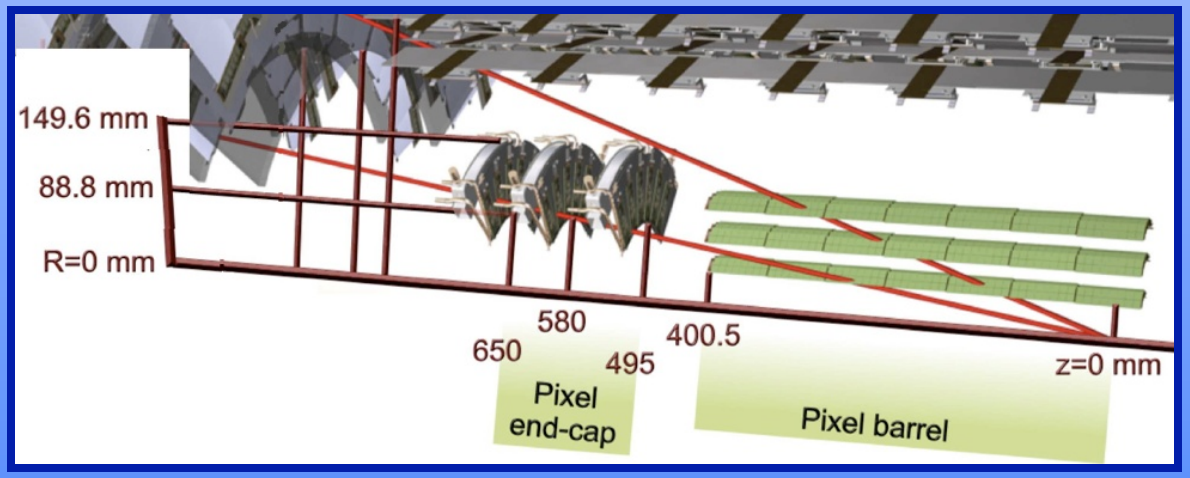

- **Three barrel layers:**
  - R= 5 cm (B-Layer), 9 cm (Layer-1), 12 cm (Layer-2)
  - modules tilted by 20º in the Rϕ plane to overcompensate the Lorentz angle.
- **Two endcaps:**
  - three disks each
  - 48 modules/disk
- **Three precise measurement points up to $|\eta|<2.5$:**
  - RΦ resolution:10 μm
  - η (R or z) resolution: 115 μm
- 1456 barrel modules and 288 forward modules, for a total of 80 million channels and a sensitive area of 1.7 m^2.
  - Environmental temperature about -13 ºC

Module overview

- **Sensor**
  - 47232 n-on-n pixels with moderated p-spray insulation
  - 250 μm thickness
  - 50 μm (RΦ) × 400 μm (η)
  - 328 rows (x_{local}) × 144 columns (y_{local})
- **16 FE chips**
  - bump bonded to sensor
- **Flex Hybrid**
  - passive components
  - Module Controller Chip to perform distribution of commands and event building.
- **Radiation-hard design:**
  - Dose 500 kGy
  - NIEL 10^{15} n_{eq}/cm^2 fluence

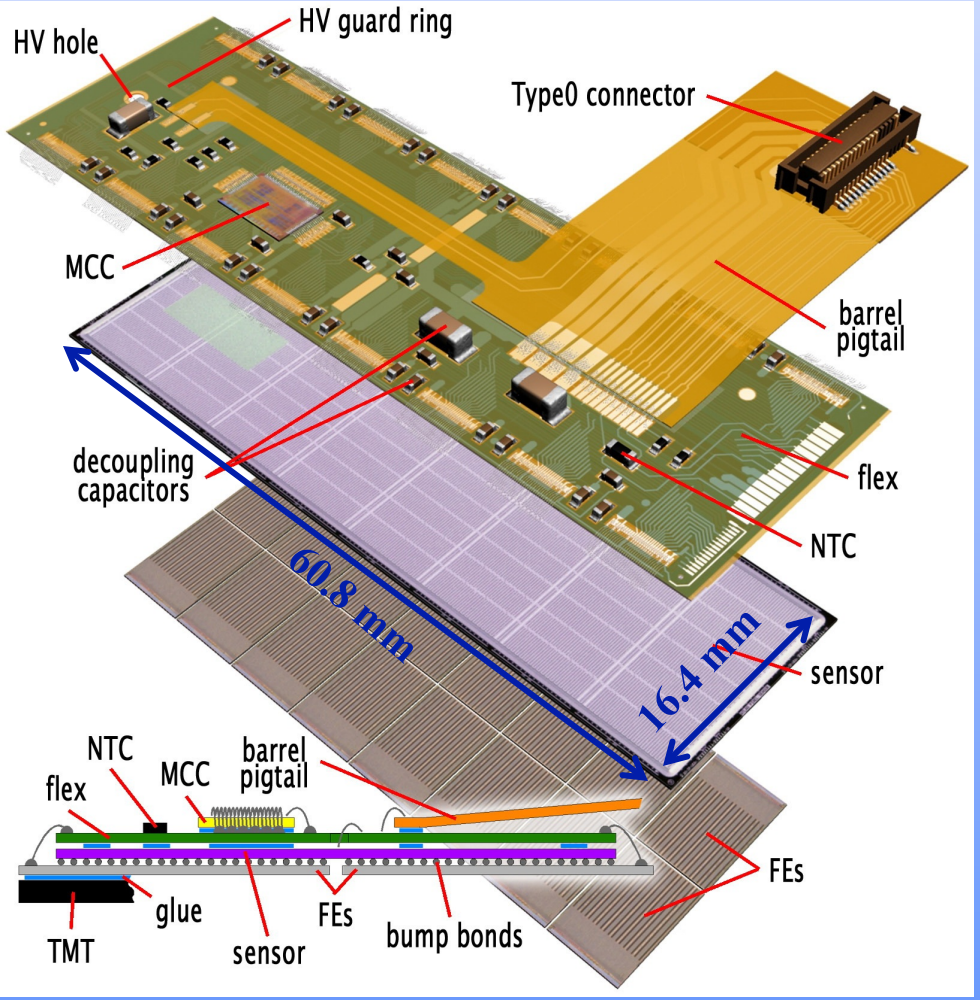

5 years at 10^{34} $cm^{-2}s^{-1}$

Structure of the pixel read-out cell

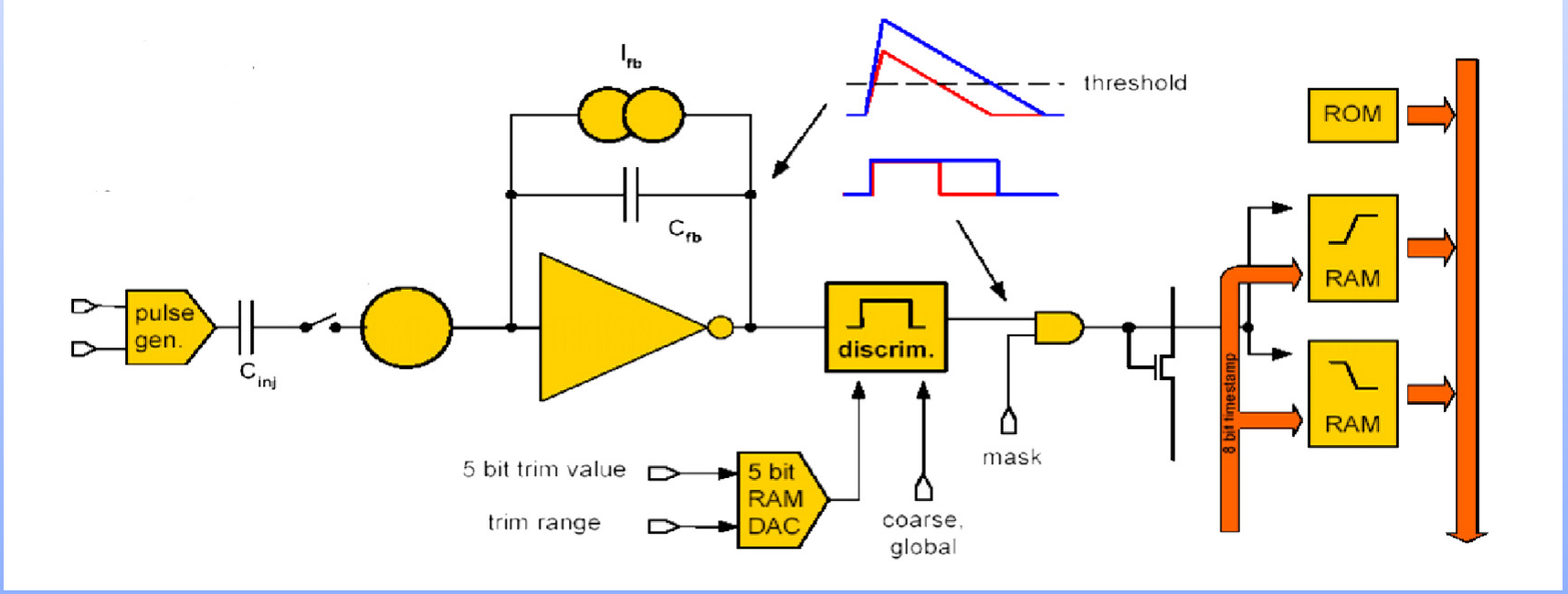

The Pixel Detector FE cell:

- a constant (adjustable) feedback current pre-amp
- a discriminator with 7 bit DAC to adjust threshold
- circuitry to measure **Time over Threshold** (ToT)
- analog and digital injection points for calibration

End of Column:

- storage of hits during the Level-1 trigger latency time
- 64 memory buffers for each column pair of 2×160 pixels
- **pixel ID + timestamp + ToT**

Optical links

A module is connected to the external world via a **low mass cable** providing all the required services:

- Bias: HV + analog and digital LV
- Temperature measurement
- Clock, serial command and data output lines

Data connection between on- and off-detector readout electronics is through an **optical link**.

Each link can be tuned by setting:

- signal phase
- threshold

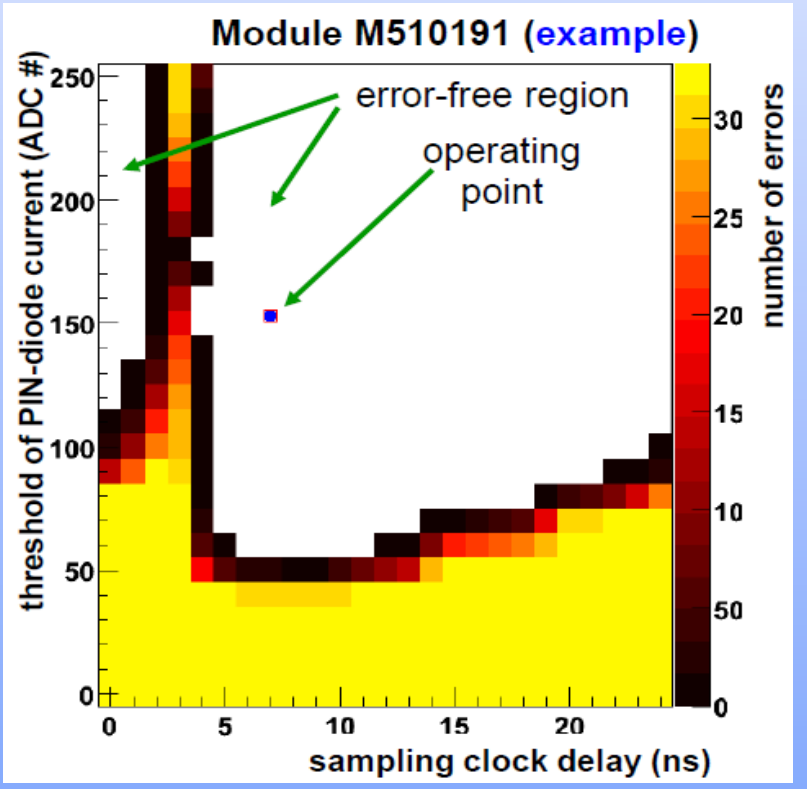

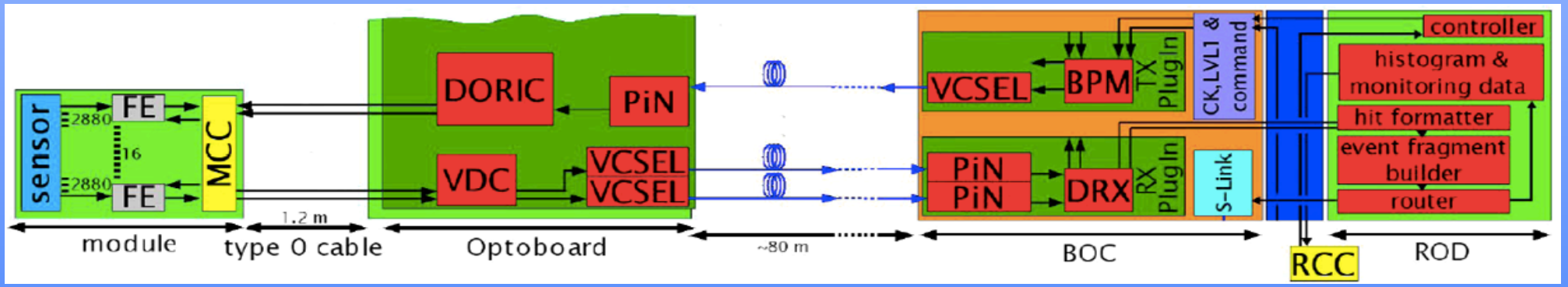

Calibration procedures

Given the enormous number of channels and free parameters to tune, the read-out electronics and the DAQ software were designed with particular attention to the calibration procedures.

Using the **internal front-end electronics self-test and charge injection capabilities**:

1. **Tune the custom rad-hard opto-link parameters** to guarantee error free data transmission.
2. **Adjust the discriminator threshold of each channel** to minimize threshold dispersion.
3. **Measure the noise** of each channel.
4. **Tune the time-over-threshold**.

Calibration procedures

Given the enormous number of channels and free parameters to tune, the read-out electronics and the DAQ software were designed with particular attention to the calibration procedures.

Using the **internal front-end electronics self-test and charge injection capabilities**:

1. **Tune the custom rad-hard opto-link parameters** to guarantee error free data transmission.
2. **Adjust the discriminator threshold of each channel** to minimize threshold dispersion.
3. **Measure the noise** of each channel.
4. **Tune the time-over-threshold**.

- Threshold and noise are determined by measuring the discriminator response as a function of the injected charge.
- The **Pixel Detector** is operated at **3500 *e* threshold**, with a dispersion of few tens of electrons.

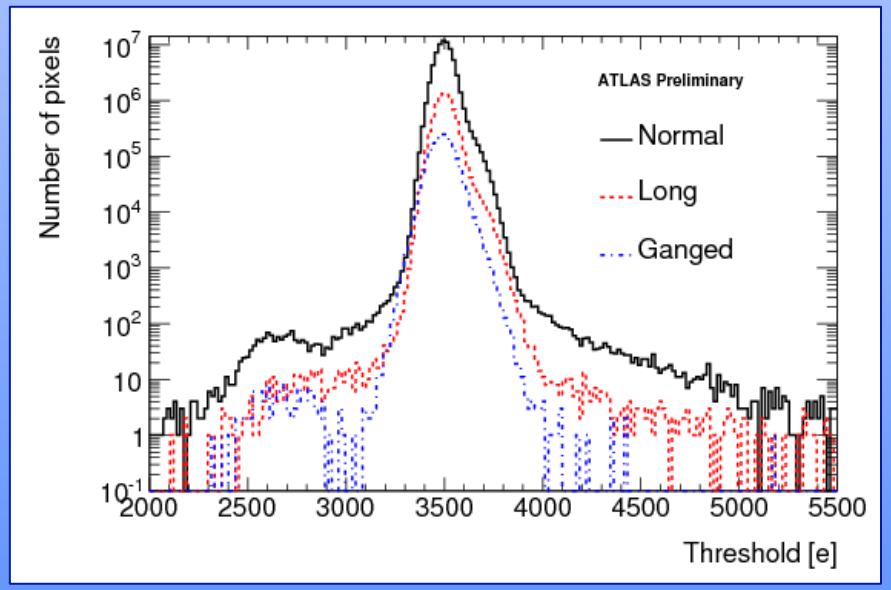

Calibration procedures

Given the enormous number of channels and free parameters to tune, the read-out electronics and the DAQ software were designed with particular attention to the calibration procedures.

Using the **internal front-end electronics self-test and charge injection capabilities**:

1. **Tune the custom rad-hard opto-link parameters** to guarantee error free data transmission.
2. **Adjust the discriminator threshold of each channel** to minimize threshold dispersion.
3. **Measure the noise** of each channel.
4. **Tune the time-over-threshold**.

- The typical **noise** of normal size pixels is **below 200 *e***.

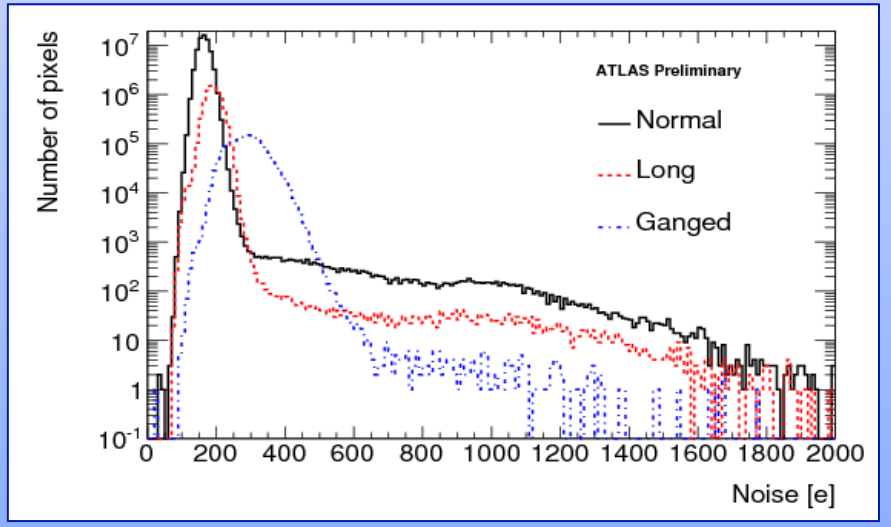

- The **large signal over noise ratio** guarantee a good stability margin even for the pixels at the edge of the array. A lower threshold (2000 *e* or even below) could be used if needed.

Calibration procedures

Given the enormous number of channels and free parameters to tune, the read-out electronics and the DAQ software were designed with particular attention to the calibration procedures.

Using the **internal front-end electronics self-test and charge injection capabilities**:

1. **Tune the custom rad-hard opto-link parameters** to guarantee error free data transmission.
2. **Adjust the discriminator threshold of each channel** to minimize threshold dispersion.
3. **Measure the noise** of each channel.
4. **Tune the time-over-threshold**.

- The pixel read-out cell can measure (in 25 ns units) the time the discriminator input remains over threshold. This is correlated with the **deposited charge**.
- The pixel cell pre-amp feedback current can be adjusted **to equalize the ToT response**.

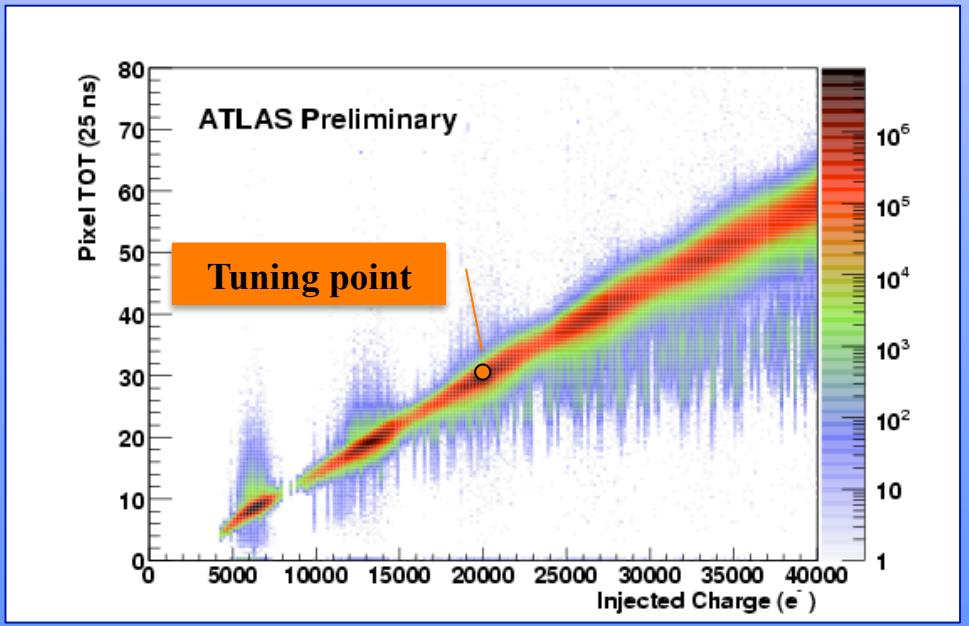

Noise occupancy and efficiency

- The occupancy due to noise can be calculated from the noise measured with the charge injection, or derived directly with a random trigger.
- The agreement between the two methods is good and the occupancy per pixel/BC is below **~10^{-9}**, masking less than 0.02% of the pixels.
- The hit efficiency of each silicon layer can be measured performing a track fit without that layer and looking for hits aligned with the resultant tracks. Typical **hit inefficiencies** are of the order of **0.2%**.
  (excluding the effect of dead modules)

- The Pixel Detector is the primary tool for **selecting primary vs. secondary particles** (converted photons for example) and **suppressing fake tracks**.

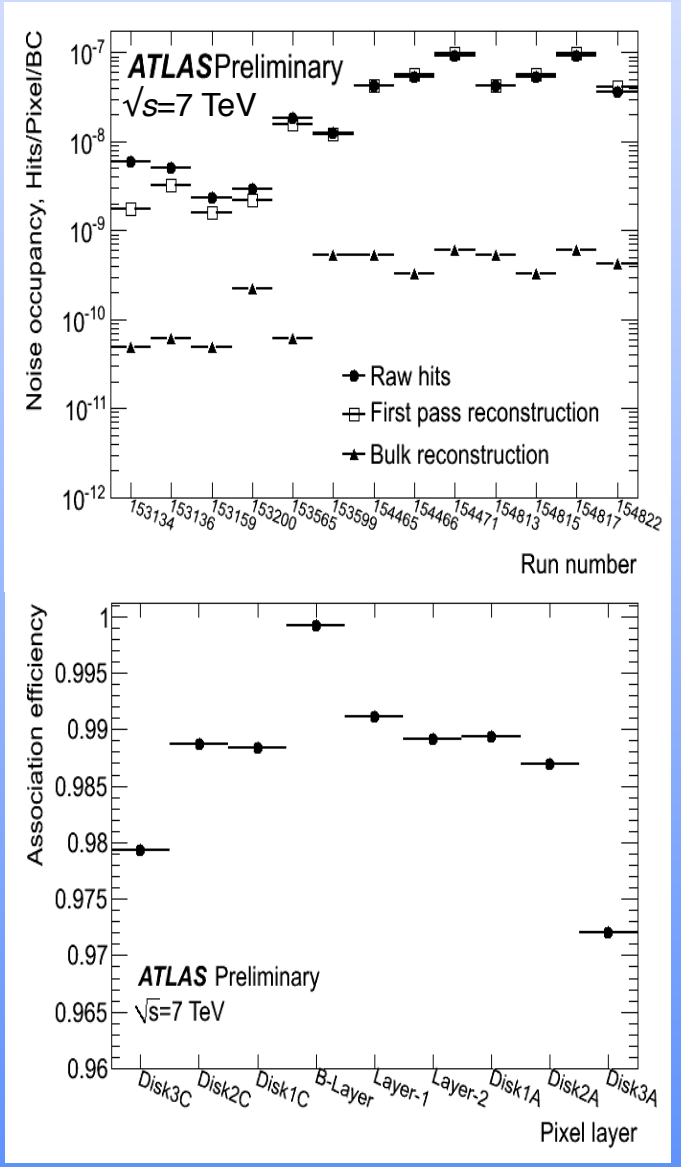

Detector status in 2012

- Currently **77 non operable modules** (out of 1744, i.e. 4.4%)
- In **2008**, after the installation, we had **25 non operable modules**. So, in average, we have a failure increase of 0.6-0.7% per year. Outermost layer seems to be more fragile.
- **Failures are highly correlated with cooling stops**. We tried to reduce the thermal shock whenever possible.
- Not always possible to identify the exact reason for the malfunctioning. Most common failures are **broken wire-bonds** or **dark optical links**.
- **Very stable operation:** fully efficient D(A)Q

ATLAS p-p run: April-June 2012

Inner Tracker			Calorimeters		Muon Spectrometer				Magnets	
Pixel	SCT	TRT	LAr	Tile	MDT	RPC	CSC	TGC	Solenoid	Toroid
100	99.6	100	96.2	99.1	100	99.6	100	100	99.4	100

All good for physics: 93.6%

Luminosity weighted relative detector uptime and good quality data delivery during 2012 stable beams in pp collisions at $\sqrt{s}$=8 TeV between April 4th and June 18th (in %) – corresponding to 6.3 fb^{-1} of recorded data. The inefficiencies in the LAr calorimeter will partially be recovered in the future.

Module failures by layer

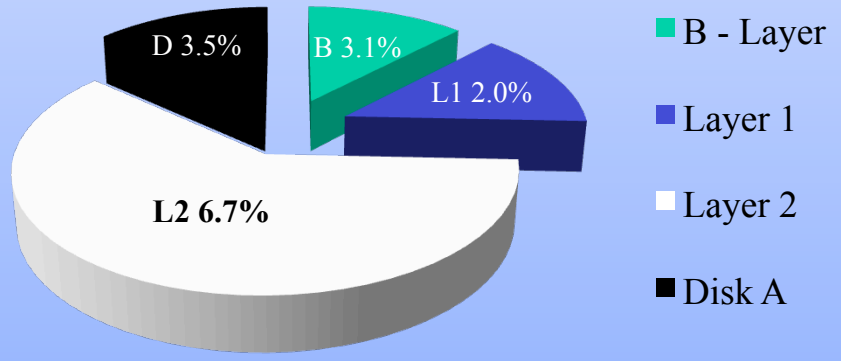

Module failures by type

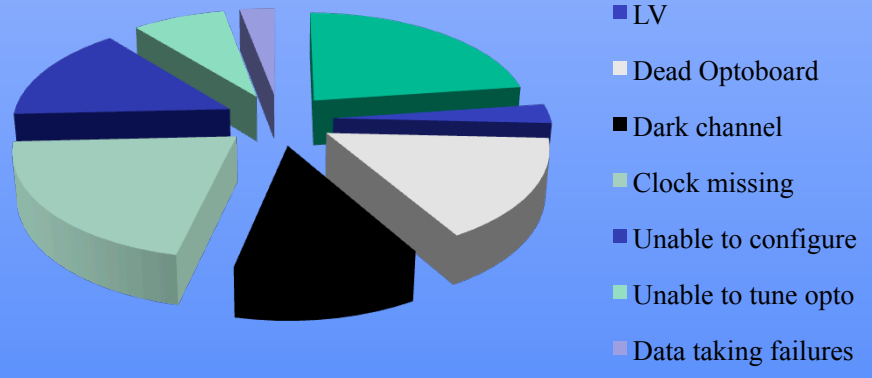

Read-out capabilities

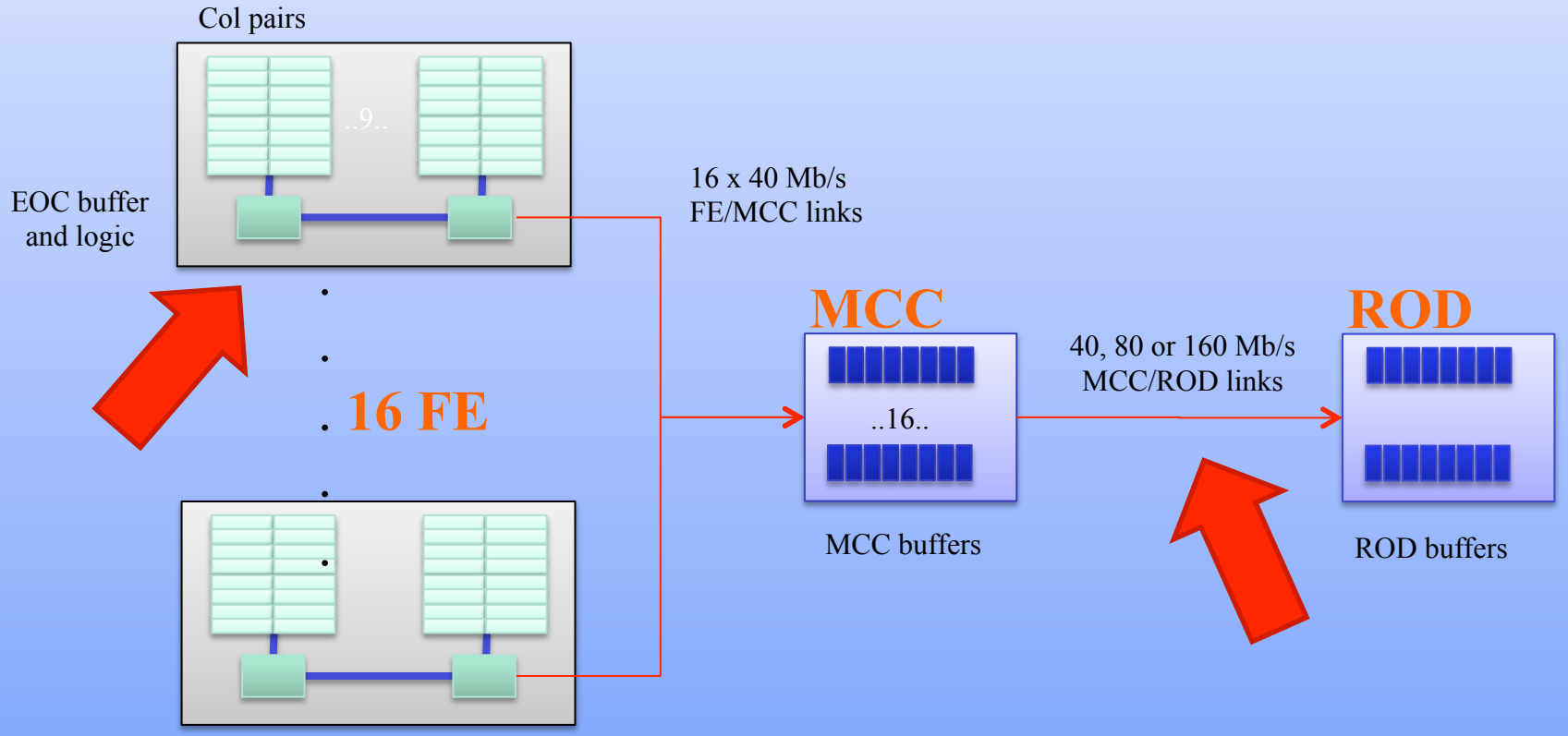

- Many elements in the read-out chain, and, in particular conditions, **each buffer or link can be saturated**.
- **The MCC/ROD link is a weak element**, especially for the outermost layer which is connected at 40 Mb/s.
- The **end of column buffers** will saturate at pixel occupancies around 1.6 10^{-3}.

Occupancy extrapolation

The Pixel Detector is now **operating in a very reliable way at 7 10^{33}cm^{-2}s^{-1} @ 50 ns**. But after the shutdown LHC luminosity will increase. Extrapolations of the expected occupancies due to minimum bias are done for 3 LHC luminosities: **1, 2 and 3 10^{34} cm^{-2}s^{-1}@ 25 ns** (2015-2017).

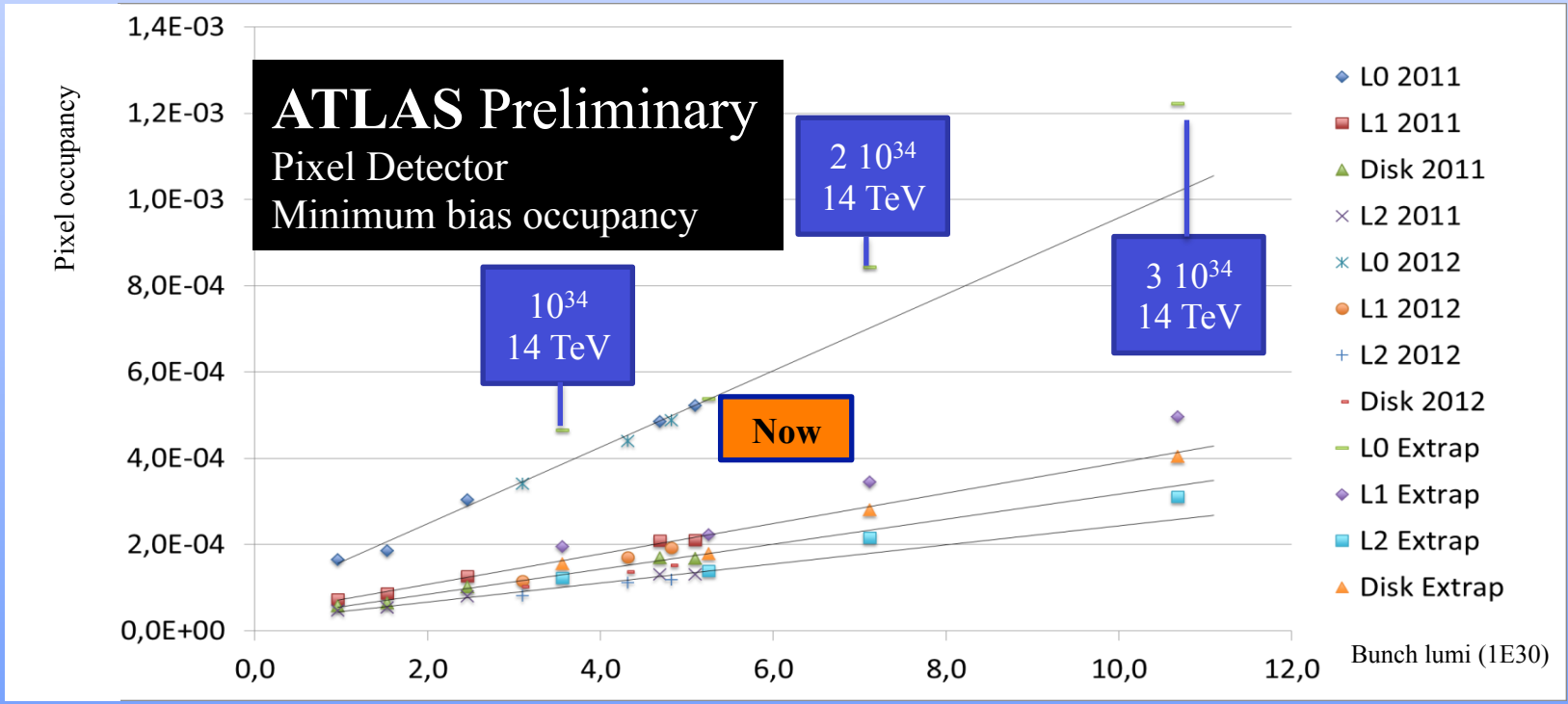

For the 2015-2017 points we assume **(13) 14 TeV**, so the occupancies are scaled **up by 20%** to take into account the increase in minimum bias cross section. We can see that **today's occupancy is larger than the one expected at design luminosity**. But even at **3 times the design luminosity**, the occupancy looks **tolerable for the read-out system**.

Facing high luminosities

- The Pixel Detector was **designed for $10^{34}cm^{-2}s^{-1}$**, but extrapolations of the present running conditions indicate **the it can be operated at 2-3 $10^{34}cm^{-2}s^{-1}$**.
- We **are continuously improving our procedures** to maximize data taking efficiency and minimize the risk of permanent damage.
- **Specific tuning** (e.g. higher threshold or faster shaping time) could be **beneficial at high luminosity** (possibility to reduce the load on the read-out system at the expense of the track quality).

- One aspect that is potentially dangerous as the luminosity increases is **the effect of SEU**, that are clearly visible even now. For example, we observe an increased rate in module de-synchronizations at the beginning of each LHC fill. We are exploiting all the capabilities of the read-out electronics to **detect and correct these effects in real-time**.

Synchronization errors vs run time

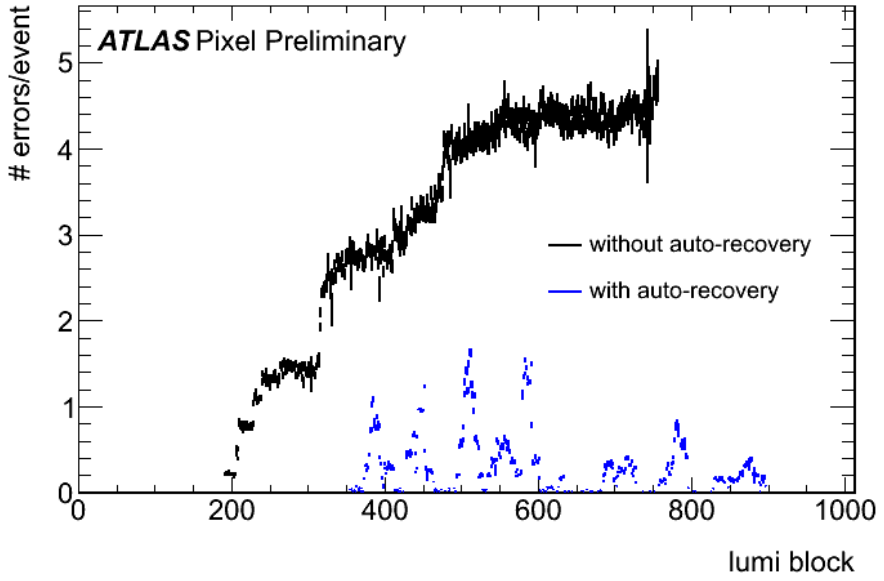

Radiation damage

- The sensors of the ATLAS Pixel Detector were designed to be still operational after a fluence of 10^{15} n_{eq}/cm^2.
- That would correspond to ~300 fb^{-1} of integrated luminosity for the innermost layer.
- Today, at ~15 fb^{-1}, the detector is still in its infancy...

- But effects are starting to be measurable:
  - **Increase of leakage current**
  - **Depletion voltage**

See Andree Schorlemmer's poster for more details about radiation damage

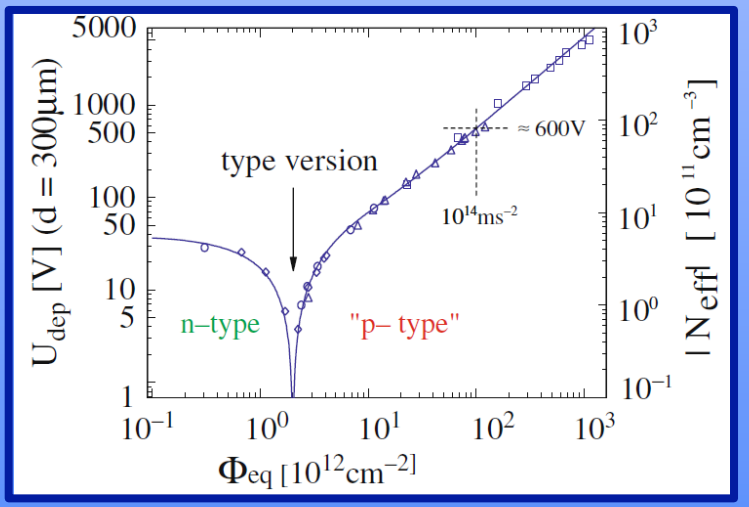

Leakage current measurements

Three available tools:

1. With the **power supply**, per **group of 6/7 modules**, with a precision of **~80 nA**.
2. For a single modules, with **dedicated hardware**. The precision is **~10 nA**, available for a limited number of modules.
3. At the **pixel level**, with a specific feature implemented in the FE chip. Useful in particular to **map non homogeneous current distributions**.

The three methods agree well, and clearly show the **increase with luminosity and the effect of the annealing**.

Predictions based on the "Dortmund" model (O. Krasel) underestimates the data by 15-25%.

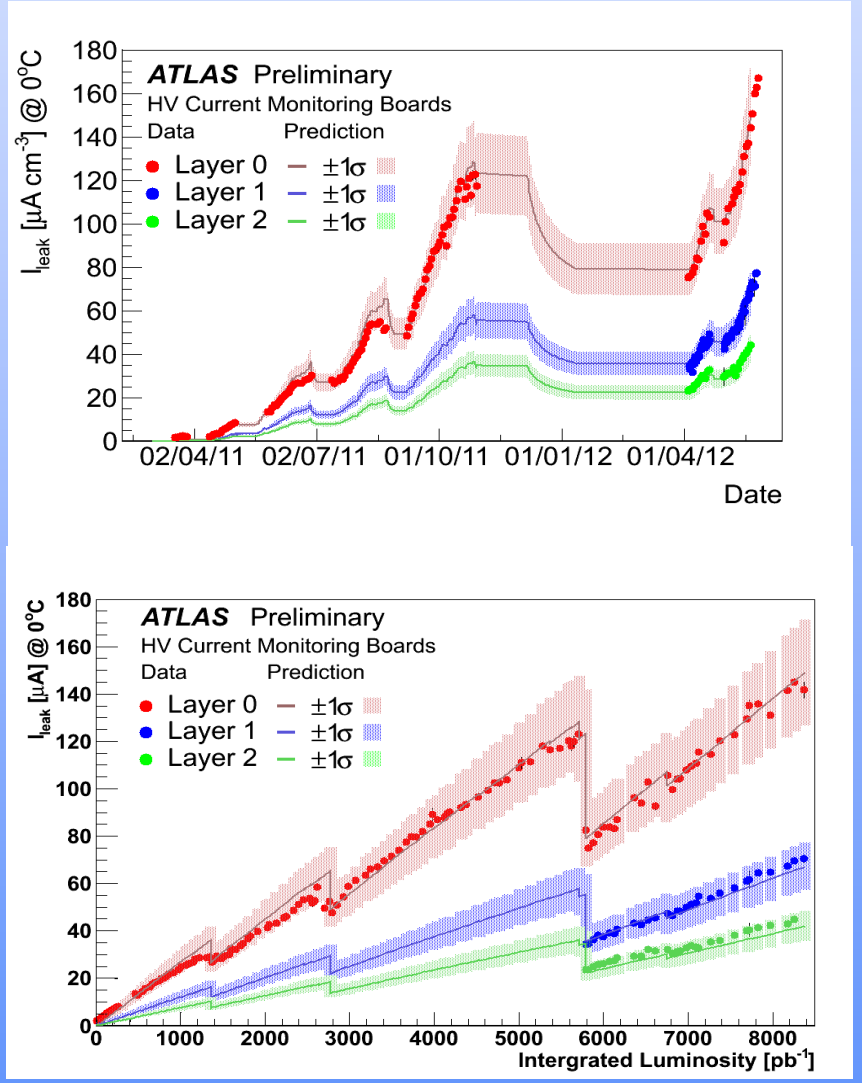

Depletion voltage measurement

- Before type-inversion, can be measured looking at the **pixel cross-talk during a voltage scan**, as the undepleted region creates a resistive path.
  - Number of pixels showing cross-talk hits decreases with increasing HV
  - Sensor structures are visible near full depletion.
- **The depletion voltage decreases with the accumulated dose**, as we are about type-inversion for the innermost layer.
- The **annealing effect** due to cooling stops is clearly visible.
- **The depletion depth can also be measured off-line**, correlating the track incidence angle with the cluster size.

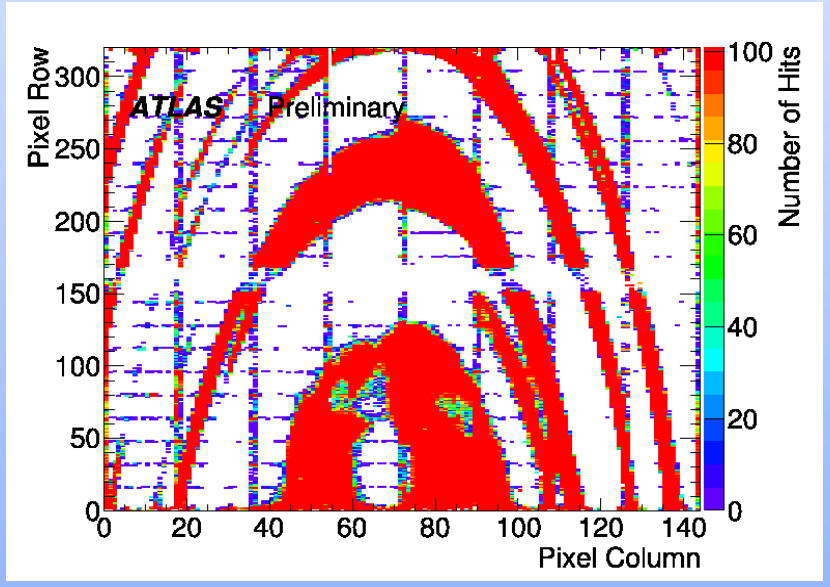

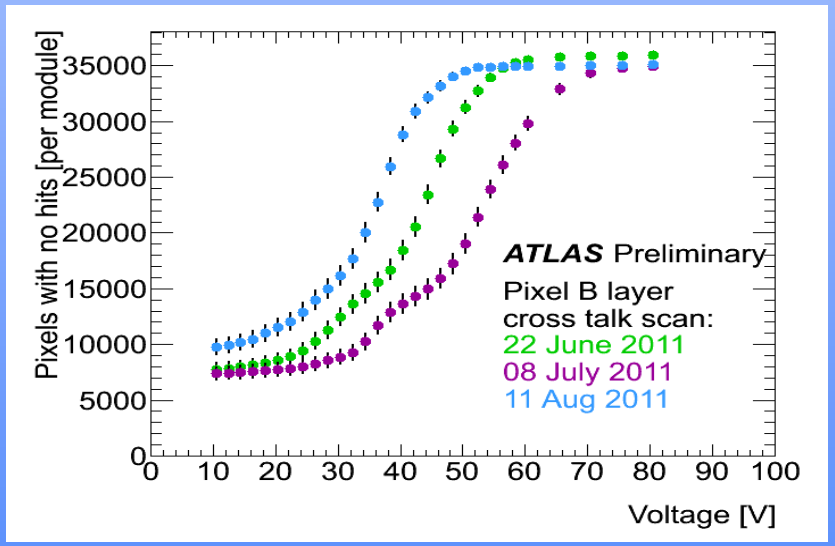

Position reconstruction

- If particles leave signal in more than one pixel, **the point resolution can be improved,** with respect to a simple geometric center of cluster, **using the pulse height** measurements.
- **Classical approach:**
  - **Charge sharing variables:**

$$\Omega_x = \frac{Q_{\text{last row}}}{Q_{\text{first row}} + Q_{\text{last row}}} \qquad \Omega_y = \frac{Q_{\text{last column}}}{Q_{\text{first column}} + Q_{\text{last column}}}$$

  - **Cluster position correction:**

$$(x_c, y_c) \rightarrow \left[x_c + \Delta_x(\Omega_x - 1/2), y_c + \Delta_y(\Omega_y - 1/2)\right]$$

- Cluster may assume complex structures:
  - Ovelapping particles, in high density environments (core of jets)
  - δ-ray production or hadronic interactions
  - **Need to fully exploit the detector information.**

Two very near particles

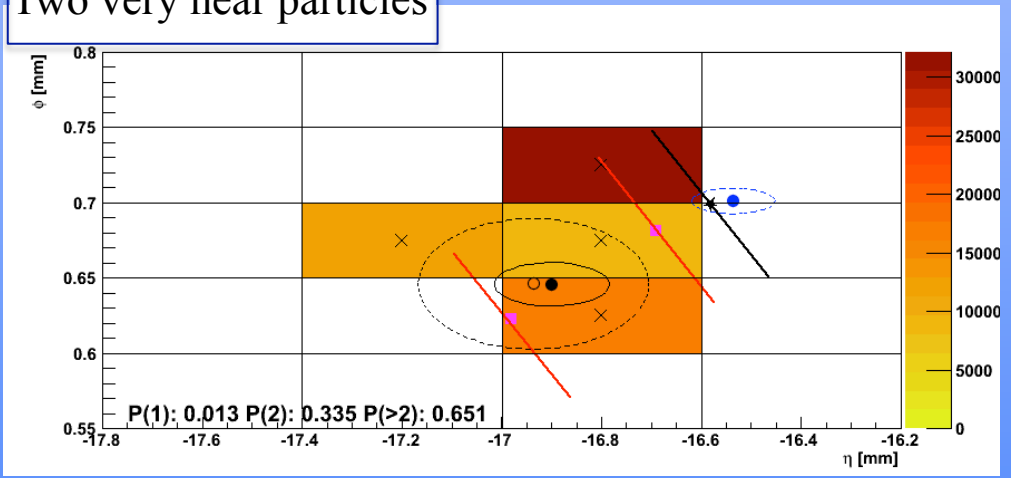

See the neural betwork reconstruction poster for more details about position resolution

Neural network processing

- A neural network is used to process the full cluster shape:
  - Recognizes hits from multiple particles
  - Non-linear interpolation of charge distribution.
- Trained on simulation of high density events:
  - $t\bar{t}$
  - High p_T-jets
- Very significant improvement in performance:
  - **Recover tails** in cluster position.
  - **Reduced by an order of magnitude the ambiguities** in cluster-to-track association
  - Recovery of tails and improved association efficiency results in **15% improvement** in impact parameter resolution.

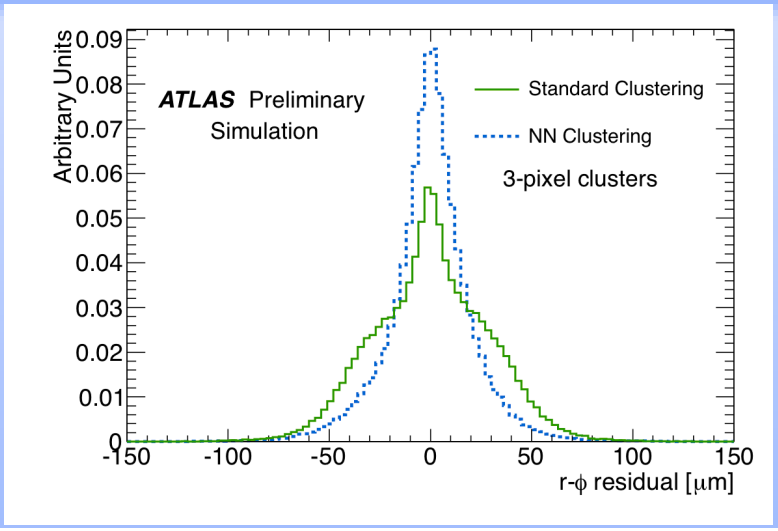

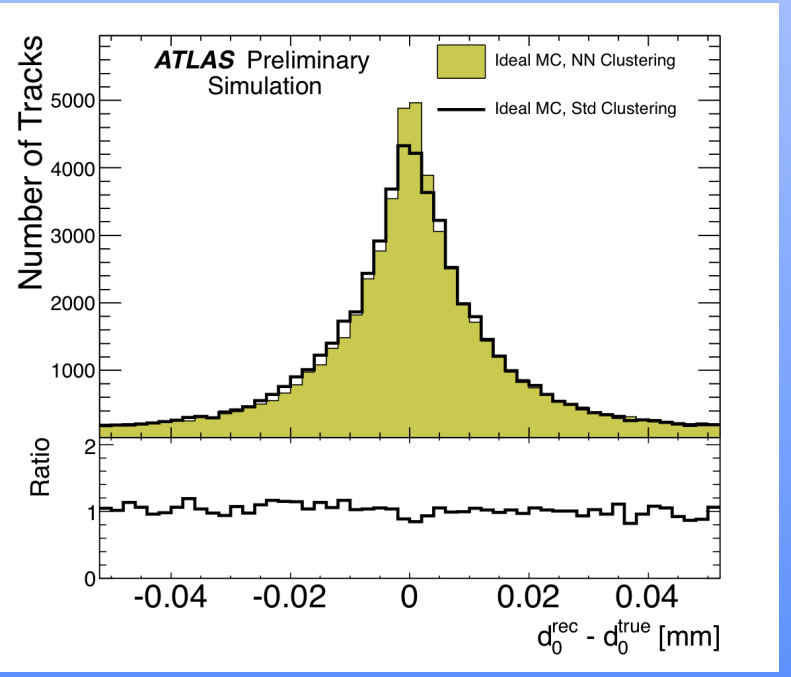

Impact parameter resolution

- Impact parameter is used to discriminate primary from secondary particles.
- Key ingredient in the reconstruction of heavy flavours (b, c, τ)
- Resolution is dominated by the first measurement on track.
  - At high p, **intrinsic detector resolution** and **alignment**.
    10 µm resolution in barrel region
  - At low p, **detector material**.
    Material effects extremely well described.

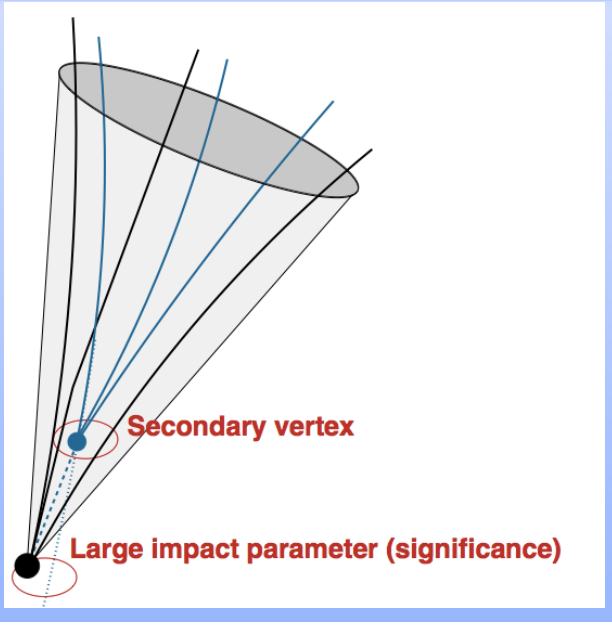

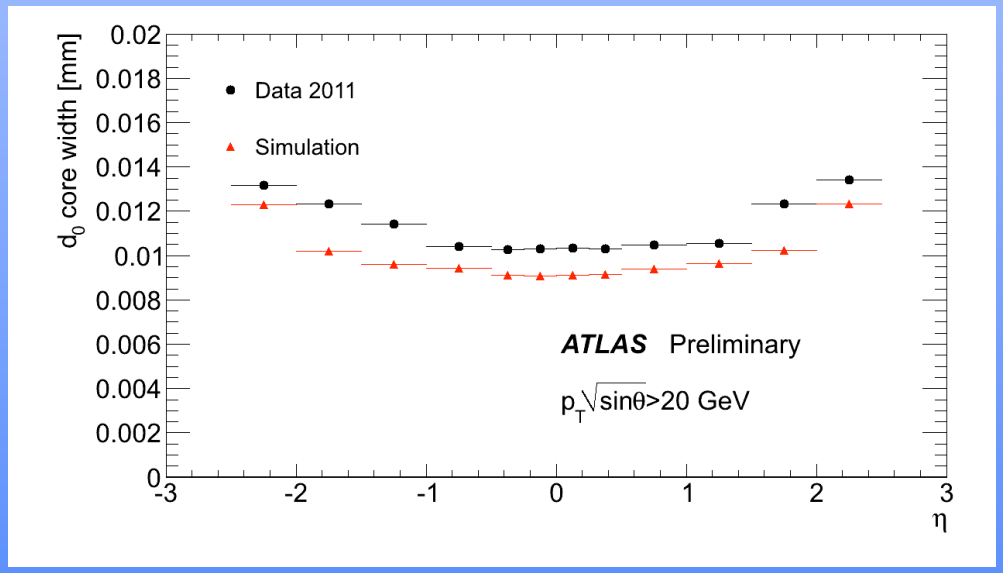

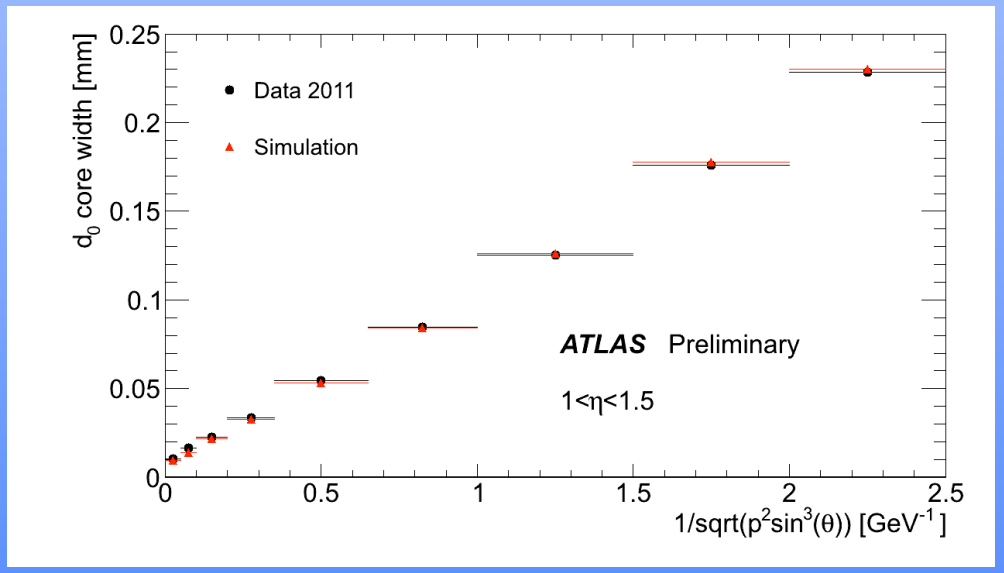

Summary and perspectives

The performance of the ATLAS Pixel Detector has been extremely satisfactory in the first years of LHC data taking:

- Meeting or **even exceeding** design specifications.
- Since the very beginning of data taking (with cosmic rays in 2008), the detector has been operating in a stable and smooth way, delivering high quality data.
- Coping well with the increasing occupancy and luminosity by a steady improvements of DAQ, calibration and data reconstruction.
- Radiation effects are observable, but matching expectations.

We expect the detector to operate well during the whole LHC phase 1, i.e. up to 2017. Some improvement is however needed…

Preparing for the next steps during the 2013-2014 LHC shutdown

- See Ole's talk for the status of the 4th layer of the ATLAS Pixel Detector (IBL).
- The extraction of the detector for the installation of new service panels is under study:
  - Allows the recovery of some dead modules.
  - Improves the performance at high luminosity.

BACKUP

Pixel types

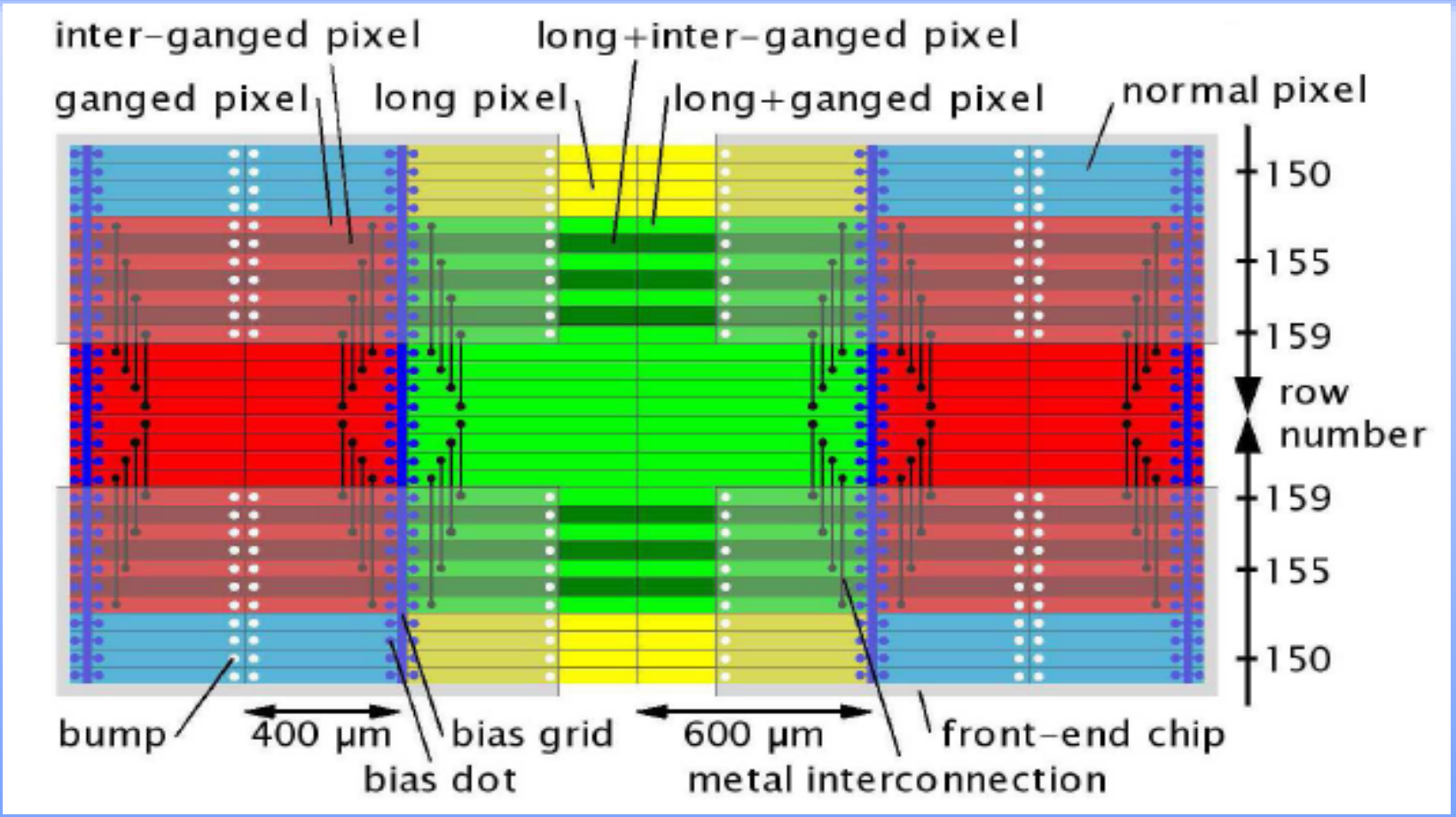

- For ganged pixels, the spacing in the inter-chip region and in the chip-edge regions are different:
  for multiple-pixel clusters it is possible to disentangle in which region it was generated.

dE/dx at work

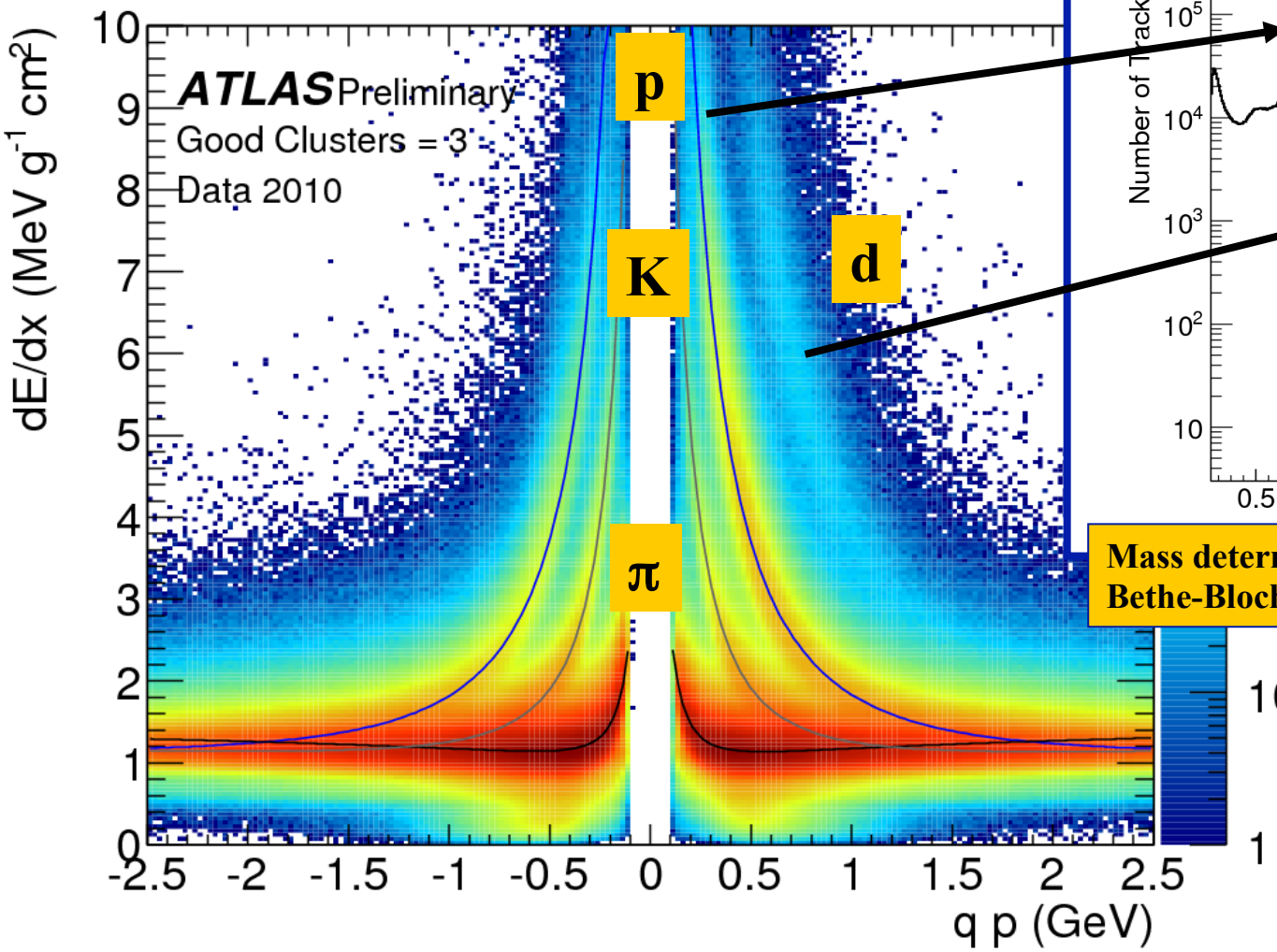

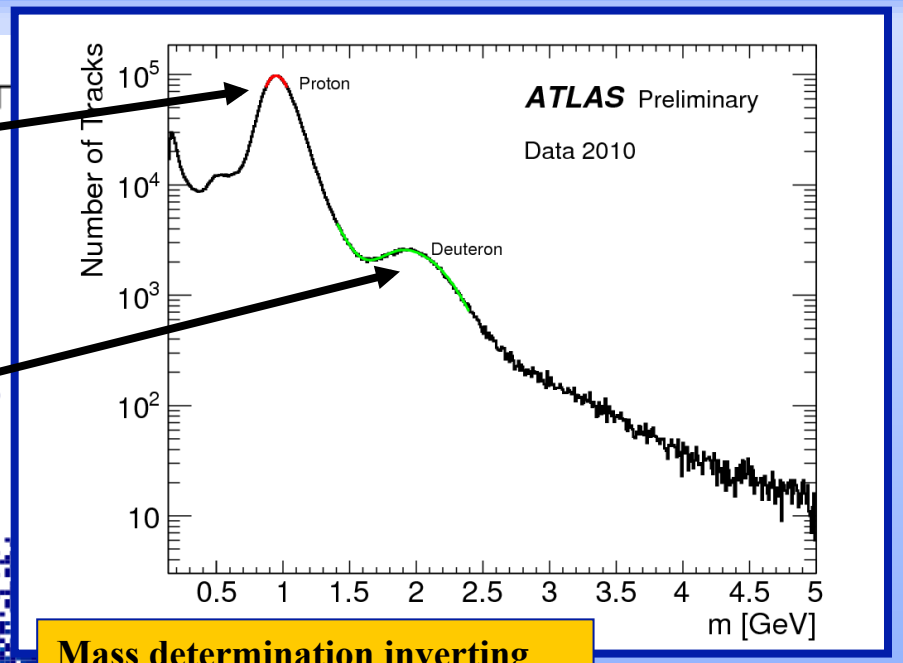

Mass determination inverting Bethe-Bloch energy loss relation

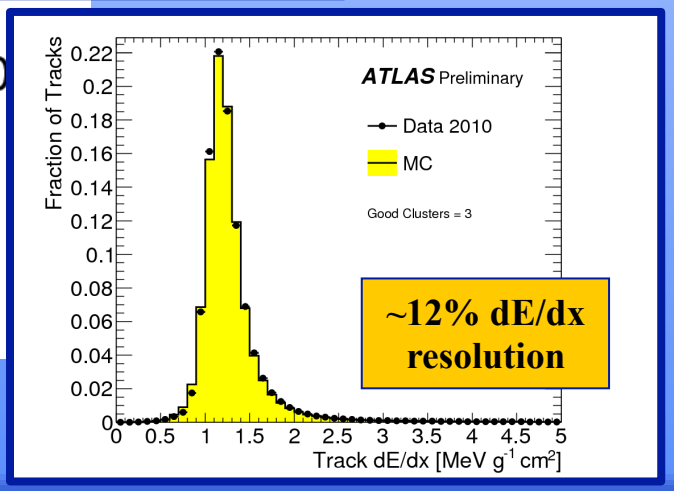

~12% dE/dx resolution

Hadro-graphy

- Material mapping usually performed by photon conversions

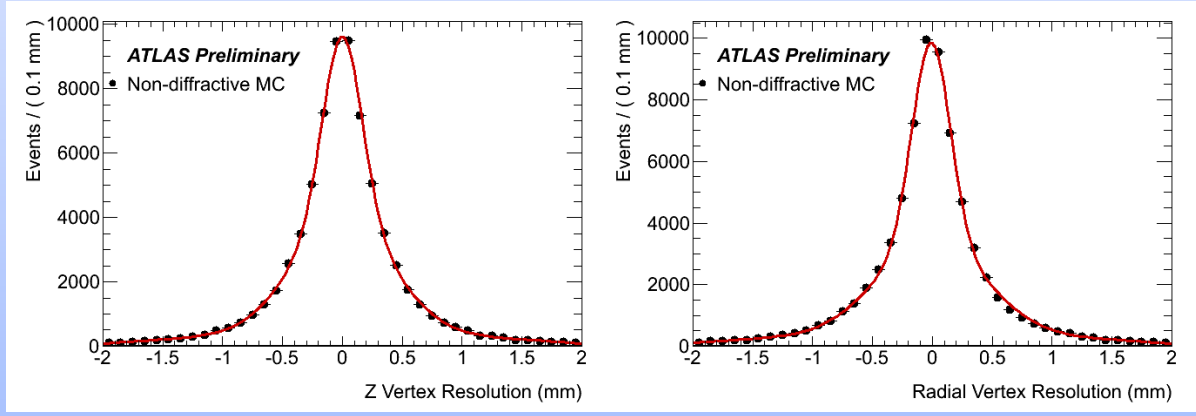

- Hadronic interactions can reach a better position resolution:
  - larger opening angle
  - σ=160 μm at Layer-0
- Very accurate detector mapping!

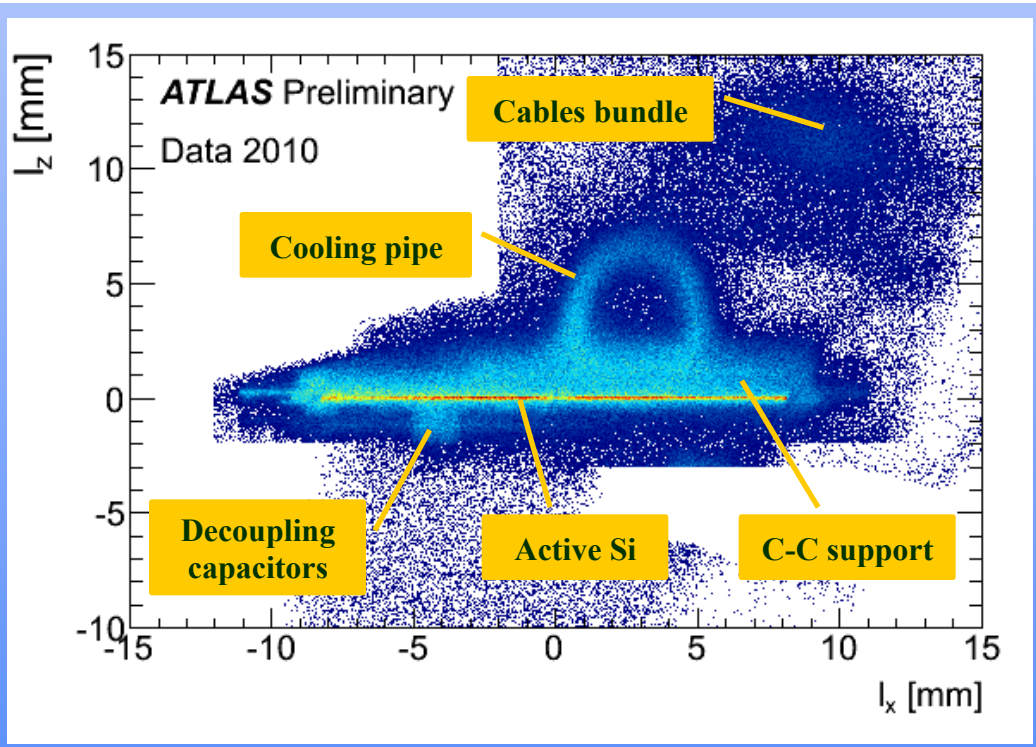

- Applications:
  - Average λ_I measurement
  - Positioning of non-sensitive material (beam pipe, support structures)